International Journal of Scientific & Engineering Research, Volume 5, Issue 10, October-2014
ISSN 2229-5518

Detect of Polymeric Nanoparticles Size Using Laser Speckle Interferometry Technique

H. El Ghandoor[1], M. A. Saudy[1], N. Zaki[2], and A. Samir[1]

[1]*Physics Department, Faculty of Science, Ain Shams University, Abbasia, 11566, Cairo, Egypt;*

[2]*Pharmaceutics Department, Faculty of Pharmacy, Ain Shams University, Abbasia, 11566, Cairo, Egypt*

E-mail- **mahssaudy@yahoo.com**

Abstract— A new double aperture laser speckle interferometry technique is presented for detecting the size of polymeric nanoparticles, namely chitosan polymer. The optical setup uses a He-Ne laser for the source together with a lens to expand the laser beam and double apertures illuminating through both of them the same scattering surface. CCD camera provides images of the two superimposed speckle fields through the double apertures, interference fringes are formed within the speckle pattern, where the images of the two apertures overlap. Thus a periodic grid structure is introduced within each speckle .A first exposure was taken with the absence of the specimen and a second one after introducing the chitosan polymer sample in the way to the rough surface. By simple subtraction of the two digital pictures, we obtain a moiré nano fringe pattern that gives us information about the polymeric Nanoparticles size. The laser speckle interferometry technique is use to investigate the effect of moiré' fringes on the particle size. TEM micrograph showed that the particle size of the samples is agreements with the results of Auto diluter submicron Particle sizer. The final dimension of the speckle grain size is controlled by the optical set-up. For samples with particle size smaller than the speckle grain size, the double aperture speckle interferometry should be used. The least measurable samples are the samples with particle size equal to the grid spacing formed within the speckles.

Index Terms— Speckle Interferometry, Nano-speckles, Nanoparticles

1 INTRODUCTION

CHITOSAN, the deacetylated derivative of chitin, is one of the abundant, renewable, nontoxic and biodegradable carbohydrate polymers, and available largely in the exoskeletons of shellfish and insects. Chitosan has been widely applied as a functional biopolymer in food and pharmaceutics. Chitosan nanoparticles have been previously synthesized as drug carriers [4-8]. Chitosan nanoparticles could elicit dose-dependent inhibitory effects on the proliferation of various tumor cell lines, while low toxicity against normal human liver cells [4, 9]. Chitosan has been used as a safe excipient in drug formulations over the last two decades [10].

The definition of laser speckle is a phenomenon in which the scattering of light from a highly coherent source, such as a laser, by a rough surface or inhomogeneous medium generates a random-intensity distribution of interfering light that gives the surface a granular appearance. Here, the random-intensity distribution results from the randomly constructive or destructive interference of the scattered coherent light rays [11-15].

Speckle interferometry (SI) is a non-contact, optical technique used in different research areas to measure the deformations of a rough object. The main interest of speckle interferometry technique was related to the non-intrusive nature of the measurement process and its high resolution and sensitivity. The standard measurement setup is based on a laser source, rough surface, and a camera that records the intensity distribution of an interference field containing the information about object deformation [16]. Speckle interferometry techniques based on the coherent addition of two speckle patterns recorded before and after the deformation of the rough object under test then a third speckle pattern is obtained from these two speckle patterns is [17-21].

In this paper a new technique for detecting the size of polymeric nanoparticles, namely -chitosan polymer- is presented. This is achieved by using the system of double – beam speckle interferometry. The optical setup uses a He-Ne laser for the source and a high resolution, (CCD) photo camera provides images of the two superimposed speckle fields through the double apertures, interference fringes were formed within the speckle pattern, where the images of the two apertures overlap. Thus a periodic grid structure is introduced within each speckle grain .A first exposure was taken with the absence of the specimen and a second one after introducing the chitosan polymer sample in the way to the rough surface. By simple subtraction of the two digital pictures, we obtain a moiré nano fringe pattern that gives us information about the polymeric Nanoparticles size. The mean size of nanoparticles was measured also by transmission electron microscope, submicron particle seizer.

2 EXPERIMENTAL WORK

2.1 Preparation of Chitosan/TPP Nanoparticles

Chitosan and sodium tripolyphosphate (TPP) nanoparticles were prepared by the ionic gelatin method where the physical cross linking by electrostatic interaction between the cationic Chitosan and the poly anion TPP which was summarized as following:

1. Chitosan was dissolved in 4.6 M HCl at concentrations 0.038%, 0.054%, 0.069% and 0.085% wt. adjusting the PH of different solutions to 4 by the addition of the appropriate volume of NaOH 0.1 M.
2. TPP was prepared as a 0.1% wt. solution in deionized water, adjusting the PH to 8 with appropriate additions of HCl 0.1 M.
3. Both solutions were filtered through a 0.22 μm pore size filter in order to remove any macroscopic material possibly present.
4. The complexation was carried out at 25^0C and under magnetic agitation (750 rpm) for a duration of 30 min, followed by sonication for 40 min, leaving then the dispersion undistributed for additional 16 h prior to any purification or analysis.
5. Dispersions with different nanoparticles content could be obtained by concentrating the dispersions during ultra-filtration and assessing their concentration by measuring the dry content after freeze drying.
6. In the final dispersion the Chitosan and TPP concentrations were therefore 0.035%, 0.05%, 0.064% and 0.079% wt.

2.2 Particle Size Measurements

2.2.1 Transmission electron microscopy (TEM)

In recent years (TEM) has been extensively used for the study of the microstructure of different samples. The sample preparation techniques and the large depth of focus of the TEM makes it very useful tool to investigate the microstructure features of our prepared sample (Chitosan). Jeol 1200 EXII transmission electron microscope is used in the present investigations.

2.2.2 Auto diluter submicron particle seizer

Auto diluter submicron Particle Seizer (75 Aero Camino, Ste. B, Santa Barbara, CA 93117) uses the dynamic light scattering principle (DLS), which also is known as photon correlation spectroscopy (PCS) or quasi-elastic light scattering (QELS).In this instrument a laser beam is directed at a suspension, in which suspended particles move in Brownian motion. Light scattered by the moving particles gives rise to interference, which affects the intensity sensed by the detector. Analysis of the intensity gives the diffusion coefficient of the particles. The diffusion coefficient, viscosity, and temperature are used in the Stokes-Einstein equation to obtain he hydrodynamic diameter of the particles.

2.3 Double-Aperture Speckle Interferometer Setup

Light from a He-Ne laser was allowed to be incident on microscope objective lens (X40), to expand the laser beam. The expanded laser beam is then incident on a collimating lens, where a plane coherent wave was obtained. This collimated coherent beam of wavelength λ=0.6328 *nm*, was allowed to illuminates a small container cell (A) made from quartz with dimensions 1 *cm* × 1 *cm* × 3 *cm* and with one face grounded to acquire a certain degree of roughness (act as a diffuser) as shown in figure 1. Two identical circular apertures (B) of *d*=0.2 *mm* in diameter and separated by a distance of *D*=4 *mm* were used adjacent to an imaging lens (C) of focal length f=15 *cm* forming two images of the speckle patterns from the rough surface with magnification ratio equals one. A high resolution CCD camera (E) was used to digitally record the image of the resultant interference grid structure.

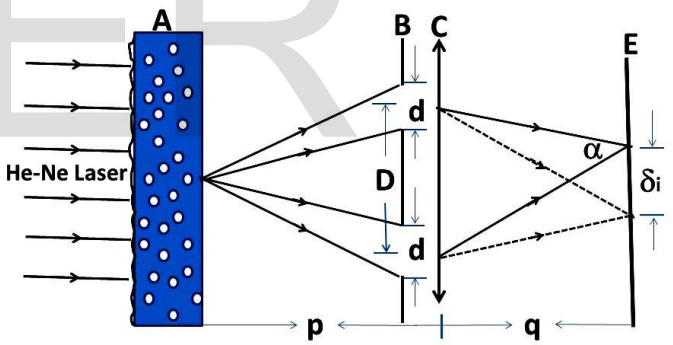

Fig.1 Double-apertures Speckle Interferometer setup. A is quartz cell filled with nanoparticle fluid with one face acts as a rough surface, B is a double apertures, C is the converging lens and E is the CCD camera.

3 THEORETICAL CONSIDERATIONS

In speckle interferometry technique, an opaque stop containing two identical small open apertures with width "*d*" and separated by distance "D" was placed in front of the imaging lens. If either of the apertures is blocked, the other forms a subjective speckle pattern image of the scattering rough surface.

When light is allowed to pass through the two apertures, each speckle pattern is modulated by Young's-type fringes, where the images of the two apertures overlap. Thus a periodic grid structure is introduced within each speckle cell of the image as shown in figure 2. The resultant

interference of grid structure Young's fringes is shown in figure 2. The figure shows that one image before introducing the liquid containing the nanoparticles, and the other image after introducing the liquid containing the nanoparticles. The grid lines run perpendicular to a line joining the two apertures centers, so that by rotating the aperture pair one can orient the grid in any direction. All the fringes observed in the grains have the same spacing, but there is no relation between the positions of the fringes when pass from one grain to another, because the phase distribution of the grains is random. The speckle resulting from the interference between the two speckle patterns produced from the double apertures, that is, the speckle pattern observed on the focal plane is modified. This new speckle pattern has no correlation with the proceeding one, but each grain is modulated by fringes.

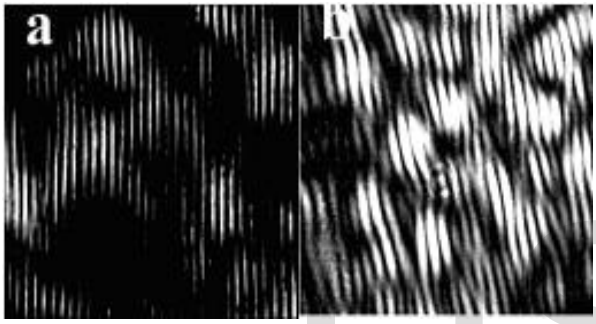

Fig. 2 The resultant interference grid structure a) before introducing the liquid containing the nanoparticles, and b) after introducing the liquid containing the nanoparticles.

The principle of measurement based on speckle interferometry consists of observing the evolution of a speckle pattern obtained by the coherence superposition of two independent fields obtained from the double apertures, as a function of the phase difference between the two fields. The relative net phase difference between both waves is [17]

$$\Delta\phi=\phi_2-\phi_1 \tag{1}$$

where ϕ_1 and ϕ_2 are the phase differences introduced from double apertures.

If a_1 , a_1' , a_2 and a_2' represent the diffracted amplitudes at a point in the image plane before and after the deformation of the object surface, the total amplitude in each state is given by

$$A=a_1+a_2, \qquad A'=a_1'+a_2' \tag{2}$$

The intensity distribution at the image plane of the CCD camera is given by

$$I=A^2+A'^2+2AA'\cos\Delta\phi \tag{3}$$

If α is the half-angle (aperture of the lens) between rays emerging from the two apertures the spacing δ_i of the grid lines is [25]

$$\delta_i=\frac{\lambda}{2\sin\alpha} \tag{4}$$

Assuming the small-angle approximation

$$\tan\alpha=\sin\alpha=\frac{D}{2q} \tag{5}$$

Taking into consideration the lens magnification $M=q/p$, where p and q are the rough object and its image distances from the lens respectively, then

$$\delta_i=\frac{\lambda Mp}{D}=\frac{\lambda q}{D} \tag{6}$$

The distance δ_i in the image plane corresponds to a distance $\delta_0=\delta_i/M$ in the object plane. Thus the apparent grid spacing in the object plane is:

$$\delta_0=\lambda(\frac{p}{D}) \tag{7}$$

Exposing the vidicon of the CCD camera in this way, twice the first before introducing the nanoparticles closer to the double- apertures, and the second after introducing the nanoparticles, then simple subtraction of the two digital pictures and making the Fourier Transformation by a computer program (image pro plus) we obtain moiré fringe pattern that gives us information about the nanoparticles dimensions. If the nanoparticles dimensions are changed the image plane alternately changes from dark to bright as the nanoparticles dimensions are equal to integral multiples of δ_0. A small local displacement of the grids in the second exposure due to introducing the nanoparticles, pleads to the formation of moiré fringes, which are contours of equal in-plane displacement, where the spacing of moiré fringes corresponds to a displacement of δ_0 given by equation (7).

If δ is the width of one speckle produced by one of the apertures alone, the number of the grid fringes that can be formed within the speckle is:

$$N=\frac{\delta}{\delta_i} \tag{8}$$

The width of one speckle grain in the image plane varies, but it can be approximated to:

$$\delta = 1.22\frac{\lambda q}{d} \qquad (9)$$

Equations (6), (8), and (9) yield

$$N = 1.22\frac{D}{d} \quad \text{for circular apertures} \qquad (10)$$

The contrast of the moiré fringes is rather low, because the random nature of the speckle pattern, where transparent areas between speckles exist. This also takes place when the scattering rough surface is translated by half a cycle of the grid spacing.

The double exposure signals can also be stored in a high resolution film, and when illuminated by a collimated coherent light beam, those areas of the image that have not been displaced or have been displaced by an integral multiple of the grid spacing will diffract light strongly in one direction, at an angle λ/δ_i corresponding to the spatial frequency of the grid. Those areas that have moved an odd-half multiple of the grid spacing contain only low spatial frequencies, centered around the zero frequency, with the highest frequency determined by the width d of the open aperture. Thus by blocking the low spatial frequencies and viewing the film at one of the diffracted orders, high contrast moiré' fringes are obtained.

For the overlapping images to produce a moiré beat over a given area of the two recorded digital signals, the spatial distribution of speckle in each signal is essentially the same. That is, a displacement of the rough surface shifts the speckle totally sideways without causing a new distribution of speckles within the image.

The distribution of the resulting speckles on the image plane is a function of the size of the double apertures and its location with respect to the rough surface as well as the relative amplitude and phase of the light distribution over the rough surface. Assuming that the size and location of the apertures remain fixed, the light distribution over the rough surface will be essentially the same before and after displacement, if the amplitude and phase of the illuminating wave remain the same. This occurs when the displacement of the rough surface is such that it displaces its imageless than a speckle width, otherwise there will be no spatial correlation between the grid structures within overlapping speckles.

4 RESULTS AND DISCUSSIONS

4.1 Particle Size Measurements

Chitosan/TPP samples (S, S, S and S) measured by (TEM) to determine their average particle size and their morphology. The micrograph of samples are shown tin figure 3. The figure shows that samples are in Nano size and their size is listed in Table 1, it is obvious that all samples are spherical in shape.

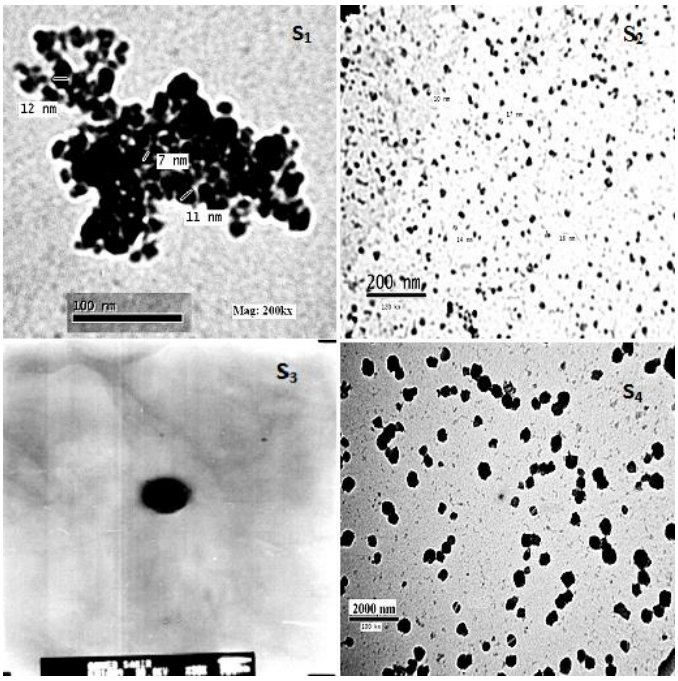

Fig. 3 Transmission electron micrograph of Chitosan/TPP samples S_1, S_2, S_3 and S_4.

The size of Chitosan/TPP samples are determined also by NICOMP™ and Auto diluter submicron Particle Seizer to be insure from the result that obtained from the (TEM), It is found that the (TEM) and NICOMP™ are very closed to each other, the particle size of the samples that is got by NICOMP™ are listed in Table 1.

Table 1
Size of Chitosan/TPP samples.

Sample	Average diameter (TEM (*nm*)	Average diameter NICOMP™ (*nm*)
S_1	10	11.8
S_2	18	21.1
S_3	145	154
S_4	320	363.4

4.2 Effect of Particle Size on Moiré Fringes

The effect of the liquid without containing the nanoparticles by recording the image of the resultant interference grid

structure before and after introducing the liquid without containing nanoparticles then we have measured different samples with different sizes by double aperture speckle interferometer as shown in figure 1. The grid spacing δ_0 was 0.075 μm= 75 nm. The speckle grain average diameter was about 450 nm, and the number of grid fringes that can be formed within the speckle is N=24.4≅24

The moiré' fringes obtained are low contrast because of the random nature of the speckle pattern, where transparent areas between speckles are projected. This also takes place when the scattering rough surface is transferred by half a cycle of the grid spacing. Fourier transform is applied for the subtraction of two grids, namely (a) before and (b) after introducing the solution with nano particles. All the steps of image processing, whether subtraction or Fourier transform, are done by using Image-pro Plus program version 4.5.0.29. The contrast of the moiré' fringes are rather low, due to the random nature of the speckle pattern, where transparent areas between speckles are obtained.

Table 2 shows the resultant interference grid structure for samples S_0 which contain no nano particles and the first image (a) obtained for empty cell and the second image (b) for the solution with nano-particle. For samples S_1, S_2, S_3 and S_4 (a) represents the resultant interference grid structure before introducing the solution containing nano-particles and (b) represents the resultant interference grid structure before introducing the solution containing nano-particles. Also 2 tables show the Subtraction of the two grids (a) and (b). The Fourier transform of the subtraction of the two grids.

From table 2, for samples S_2, S_1 and S_2, we find that when the particle size is smaller than the grid spacing the number of moiré fringes aren't changed. For sample S_3 the number of moiré' fringes are increased by two, because of the fourth sample is displaced the grids by 2 δ_o. For sample S_4 the number of moiré' fringes are increased by four, because of the fourth sample is displaced the grids by 4 δ_o. From samples S_3 and S_4, it is found that when the particle size is larger than the grid spacing the number of moiré fringes is changed.

5 CONCLUSION

Chitosan nanoparticles were produced by ion tropic gelatin of chitosan with sodium tripolyphosphate (TPP), a small ion with a triple negative charge throughout the physiologically acceptable pH range. TEM and Auto diluter submicron Particle Seizer are used to identify and study the microstructure of the prepared samples. The Double aperture speckle interferometer is used to study the effect of particle size on moiré fringes**.** TEM micrograph showed that the prepared samples are dispersed homogenously as a single particle in water acting as carrier liquid and the particle size of the samples is agreements with the results of Auto diluter submicron Particle seizer. The final dimension of the speckle grain size is controlled by the optical set-up. For samples with particle size smaller than the speckle grain size, the double aperture speckle interferometry is to be used. The least measurable samples are the samples with particle size equal to the grid spacing formed within the speckles. For a certain set-up the grid spacing is fixed, which denotes the least measurable samples which are equal to integer multiples of the grid spacing. The clear dependence of the grid spacing on the distance of the two apertures should be noted. The smaller the value of the distance the larger is the grid spacing within the speckles. On the other hand, when the grid spacing is decreased a condition may be reached where the fringes just cannot be resolved any more. This corresponds to the minimum measurement giving one moiré when the particle size is just equal to one grid spacing.

Table 2

The resultant interference grid structure for different samples.

Samples	(a) The resultant interference grid structure before introducing the solution containing nano-particles	(b) The resultant interference grid structure after introducing the solution containing nano-particles	Subtraction of the two grids (a) and (b)	Moiré fringes resulting from the Fourier transform of the subtraction of the two grids
S_0 (a) empty cell (b) solution with no nano-particle	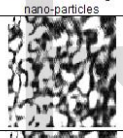	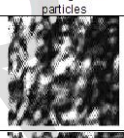	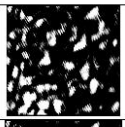	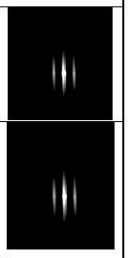
S_1 (a) solution with no nano-particle (b) the Chitosan/TPP particles with particle size (7-12) nm	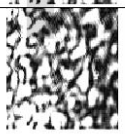	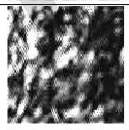	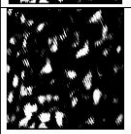	
S_2 (a) solution with no nano-particle (b) the Chitosan/TPP particles with particle size (17-23) nm	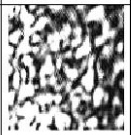	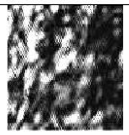	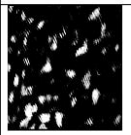	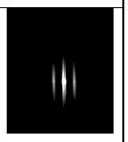
S_3 (a) solution with no nano-particle (b) the Chitosan/TPP particles with particle size (145-155) nm	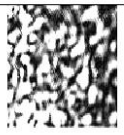			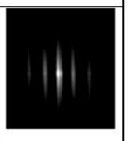
S_4 (a) solution with no nano-particle (b) the Chitosan/TPP particles with particle size (320-360) nm	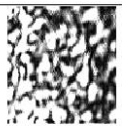	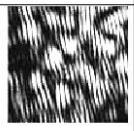	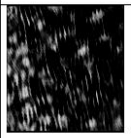	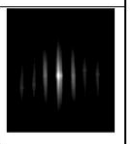

REFERENCES

[1] K. Singh, A. Mishra, "Water soluble chitosan nanoparticle for the effective delivery of lipophilic drugs", *International J. Applied Pharmaceutics*, **5**, 3 (2013) 1.

[2] L.B. Kiss, J. Söderlund, G.A. Niklasson, C.G. Granqvist, "New approach to the origin of lognormal size distributions of nanoparticles", *Nanotechnology*, **10** (1999) 57.

[3] C. Buzea, I. Pacheco, and K. Robbie, "Nanomaterials and Nanoparticles: Sources and Toxicity", *Biointerphases*, **2**, 4 (2007) MR17.

[4] L.F. Qi, Z.R. Xu, Y. Li, X. Jiang, X.Y. Han, "In vitro effects of chitosan nanoparticles on proliferation of human gastric carcinoma cell line MGC803 cells", *World J Gastroenterol*, **11**, 33 (2005) 5136.

[5] C. Qin**,** Y**.** Du, L. Xiao, Z. Li, X. Gao, "Enzymic preparation of water-soluble chitosan and their antitumor activity", *Int J Biol Macromol*, **31** (2002) 111.

[6] L. Zheng**,** J**.** Zhu, "Study on antimicrobial activity of chitosan with different molecular weights" *Carbohyd Polym*, **54** (2003) 527.

[7] Y. Pan**,** Y**.** Li, H. Zhao, J. Zheng, H. Xu, G. Wei, J. Hao, F. Cui, "Bioadhesive polysaccharide in protein delivery system: chitosan nanoparticles improve the intestinal absorption of insulin in vivo", *Int J Pharm*, **249** (2002) 139.

[8] X. YM**,** D. YM, "Effect of molecular structure of chitosan on protein delivery properties of chitosan nanoparticles", *Int J Pharm*, **250** (2003) 215.

[9] Q. LF**,** X. ZR, x. Jiang, C. Hu, X. Zou, "Preparation and antibacterial activity of chitosan nanoparticles" *Carbohyd Res*, **339** (2004) 2693.

[10] S. Senela, J. Susan, J. McClure, "Potential applications of chitosan in veterinary medicine", *Advanced Drug Delivery Reviews* **56** (2004) 1467.

[11] K.D. Kihm, "Laser speckle photography technique", *Advances in heat transfer*, **30** (1997) 255.

[12] M. Tebaldi, A. Lencina, N. Bolognini, "Analysis and applications of the speckle patterns registered in a photorefractive BTO crystal", *Opt. Commun*. **202**, (2002) 257.

[13] R.P. Khetan and F.P. Chiang, "Strain analysis by one-beam laser speckle interferometry. 1: Single aperture method", *Appl. Opt*., **15**, 9 (1976) 2205.

[14] L. Angel, M. Tebaldi, M. Trivi and N. Bolognini, "Phase-object analysis with a speckle interferometer", *Opt. Lett*. **27**, 7 (2002) 506.

[15] G.J. Tearney and B.E. Boume, "Atherosclerotic plaque characterization by spatial and temporal speckle pattern analysis", *Opt. Lett*. **27**, 7 (2002) 743.

[16] I.T. Nistea, D.N. Borza, "High speed speckle interferometry for experimental analysis of dynamic phenomena", *Optics and Lasers in Engineering*, **51** (2013) 453.

[17] R.S. Sirohi, "Speckle Metrology", Marcel Dekker, Inc. NewYork, 1993.

[18] M. Sjödahl and L.R. Benckert, "Electronic speckle photography: analysis of an algorithm giving the displacement with sub pixel accuracy", *Applied Optics*, **32**, (1993) 2278.

[19] M. Sjödahl, "Electronic speckle photography: increased accuracy by nonintegral pixel shifting", *Applied Optics*, **33**, (1994) 6667.

[20] M. Sjödahl, "Accuracy in electronic speckle photography", *Applied Optics*, **36** (1997) 2875.

[21] M. QIAN, J. Liu, Z. Shen, X. Ni, Q. Li and Y. Xuan, "Measurement of the velocities of nanoparticles in nanofluids with laser speckle velocimetry", *Laser in Eng*, **18**, (2008) 203.

[22] A. Lencina and P. Vaveliuk, M. Tebaldi, N. Bolognini, "Modulated speckle simulations based on the random-walk model", *Opt. Lett.*, **28** (2003) 1748.

[23] N. Barakat, W. Merzkirch, and H. El-Ghandoor, "Application of Speckle Pattern Photography and Speckle Interferometry to the Measurements of Zero Gradient and Constant Gradient Velocities", *Optik*, **74**, 3 (1986) 114.

[24] N. Barakat, A.M. Hamed, and H. El-Ghandoor, "Study of Fluid Flow using Speckle Interferometry", *Optik*, **76**, 3 (1987) 102.

[25] H. El Ghandoor, H. M. Zidan, M. H. Khalil, and M. I. Ismail, "Application of laser speckle interferometry for the study of $Co_xFe_{(1-x)}Fe_2O_4$ magnetic fluids", *Phys. Scr.* **86** (2012) 015403 (7pp).